

*Present address: Korea Advanced Institute of Science, P.O. Box 150, Chungryang-ri, Seoul, Korea.

¹For a review of this subject, see articles by D. Lazarus and R. W. Keyes, in *Solids Under Pressure*, edited by W. Paul and D. M. Warschauer (McGraw-Hill, New York, 1963).

²C. P. Flynn, *Phys. Rev.* **171**, 682 (1968).

³C. P. Flynn, *Z. Naturforsch.* **26a**, 99 (1971); *Point Defects and Diffusion* (Oxford U.P., Oxford, England, 1972), Chap. 9.

⁴I. D. Faux and A. B. Lidiard, *Z. Naturforsch.* **26a**, 62 (1971).

⁵W. Biermann, *Z. Physik. Chem. (Frankfurt)* **25**, 90 (1960); **25**, 253 (1960).

⁶C. B. Pierce, *Phys. Rev.* **123**, 253 (1960).

⁷W. H. Taylor II, N. B. Daniels, B. S. H. Royce, and R. Smoluchowski, *J. Phys. Chem. Solids* **27**, 39 (1966).

⁸M. Beyeler and D. Lazarus, *Solid State Commun.* **7**, 1487 (1969).

⁹M. Beyeler and D. Lazarus, *Z. Naturforsch.* **26a**, 291 (1971).

¹⁰D. Lazarus, D. N. Yoon, and R. N. Jeffrey, *Z. Naturforsch.* **26a**, 56 (1971).

¹¹R. M. Emrick, *Phys. Rev.* **122**, 1720 (1961).

¹²D. Yoon, thesis (Harvard University, 1967) (unpublished).

¹³For more detailed data, see Ref. 10.

¹⁴D. Miliotis and D. N. Yoon, *J. Phys. Chem. Solids* **30**, 1241 (1969).

¹⁵R. G. Fuller *et al.*, *Phys. Rev. Letters* **20**, 662 (1968).

¹⁶K. Kobayashi and T. Tomiki, *J. Phys. Soc. Japan* **15**, 1982 (1960).

¹⁷See A. B. Lidiard, in *Handbuch der Physik*, edited by S. Flügge (Springer, Berlin, 1957), Vol. 20, p. 246.

¹⁸D. Enck, *Phys. Rev.* **119**, 1873 (1960).

¹⁹L. Hunter and S. Siegel, *Phys. Rev.* **61**, 84 (1942).

²⁰S. P. Nikanaorov and A. V. Stepanov, *Zh. Eksperim. i Teor. Fiz.* **37**, 1814 (1959) [*Sov. Phys. JETP* **10**, 1280 (1959)].

²¹R. W. Roberts and C. S. Smith, *J. Phys. Chem. Solids* **31**, 619 (1970).

²²D. Lazarus, *Phys. Rev.* **76**, 545 (1949); R. A. Bertels and D. E. Schuele, *J. Phys. Chem. Solids* **26**, 537 (1965).

²³P. J. Reddy and A. L. Ruoff, in *Physics of Solids at High Pressure*, edited by C. T. Tomizuka and R. M. Emrick (Academic, New York, 1965), p. 510.

²⁴R. G. Fuller, *Phys. Rev.* **142**, 524 (1966).

²⁵V. C. Nelson and R. J. Friauf, *J. Phys. Chem. Solids* **31**, 825 (1970).

²⁶J. Rolfe, *Can. J. Phys.* **42**, 2195 (1964).

²⁷M. P. Tosi and F. G. Fumi, *J. Phys. Chem. Solids* **25**, 31 (1964); **25**, 45 (1964).

²⁸B. Fritz, F. Luty, and J. Anger, *Z. Physik* **174**, 240 (1963).

²⁹C. Zener, *Acta Cryst.* **2**, 163 (1949).

³⁰H. Brooks, *Impurities and Imperfections* (American Society for Metals, Cleveland, 1955).

³¹L. W. Barr and A. B. Lidiard, *Physical Chemistry, an Advanced Treatise* (Academic, New York, 1970), Vol. 10.

³²S. A. Rice, *Phys. Rev.* **112**, 804 (1958); O. P. Manley, *J. Phys. Chem. Solids* **32**, 1046 (1960).

³³C. Postmus, J. R. Ferraro, and S. S. Mitra, *Phys. Rev.* **174**, 983 (1968).

³⁴For a brief review, see Ref. 4.

Radiation-Induced $[\text{Na}]^0$ Centers in MgO and SrO[†]

M. M. Abraham, Y. Chen, J. L. Kolopus,* and H. T. Tohver[‡]

Solid State Division, Oak Ridge National Laboratory, Oak Ridge, Tennessee 37830

(Received 9 February 1972)

Substitutional monovalent sodium ions in MgO and SrO trap holes when exposed to ionizing radiation at 77 K. The $[\text{Na}]^0$ centers thus formed have $\langle 100 \rangle$ axial symmetry at 4.2 K and their spin-Hamiltonian parameters are reported. The isotropic part of the hyperfine interaction for $[\text{Na}]^0$, which has opposite sign to the anisotropic term, is larger than that observed for $[\text{Li}]^0$ in these hosts. Optical absorption bands have been correlated with the $[\text{Na}]^0$ centers, and their peaks occur at 1.58 eV for MgO and 1.34 eV for SrO. Decay temperatures have been determined to be approximately 190 K for MgO and 160 K for SrO. The EPR, optical, and thermal properties of these centers resemble those of the V^- and $[\text{Li}]^0$ centers.

INTRODUCTION

During irradiation a cation vacancy in the alkaline earth oxides can trap a hole and form the paramagnetic V^- center.¹⁻³ The center has been identified by EPR studies to have axial symmetry along the $\langle 100 \rangle$ direction, with the hole preferentially located at one of the neighboring oxygen sites, forming an

O^- ion, at any given time. In the case of MgO, an optical absorption band peaking at 2.3 eV has been correlated with the V^- center.^{4,5} The half-width of the band, ~ 1 eV, is exceptionally large and the oscillator strength of ~ 0.1 reflects neither a purely allowed nor a purely forbidden transition.

A monovalent alkali ion placed at a cation vacancy can also capture a hole during irradiation to form

a paramagnetic, but neutral, $[M]^0$ center. The two types of centers, the V^- and the $[M]^0$, are expected to be basically the same in optical properties and symmetry, both of which arise from essentially O^- -ion wave functions. $[\text{Li}]^0$ centers in MgO , CaO , and SrO ,^{6,7} and $[\text{Na}]^0$ centers in CaO ,⁷ have been studied and indeed found to have $\langle 100 \rangle$ symmetry. The band peaks of the $[M]^0$ centers were clearly shifted from those of the V^- centers, as might be expected owing to the altered charge state. The bandwidth and oscillator strength of the $[\text{Li}]^0$ center in CaO , the only such reported values for $[M]^0$ centers to date, did not differ appreciably from those of the V^- center in MgO .^{5,8} In principle, the hyperfine structure generated by the alkali nucleus in the $[M]^0$ center contains more detailed information about the hole wave functions than the structureless line of the V^- center. In this paper, we report the observation of $[\text{Na}]^0$ centers in both MgO and SrO and present optical, magnetic, and thermal properties of these centers.

EXPERIMENTAL PROCEDURES

Sodium ions were incorporated into MgO and SrO during crystal growth in an arc furnace.⁹ The starting materials were MgO powder from the Kanto Chemical Co. (Tokyo) and SrCO_3 from the Mallinckrodt Chemical Co., each mixed with about 10% Na_2CO_3 .

To generate the free holes subsequently trapped by the substitutional Na ions, single crystals of the oxides were irradiated at 77 K with either 2-MeV electrons from a Van de Graaff accelerator or ^{60}Co γ rays. The crystals were mounted into the EPR spectrometer and subsequently cooled to 4.2 K without any intervening warmup. All optical measurements were carried out at 77 K with a Cary 14 spectrophotometer, while the EPR work was performed at 4.2 or 1.5 K with both homodyne and superheterodyne spectrometers at X-band frequencies.

Isochronal-annealing experiments started with a

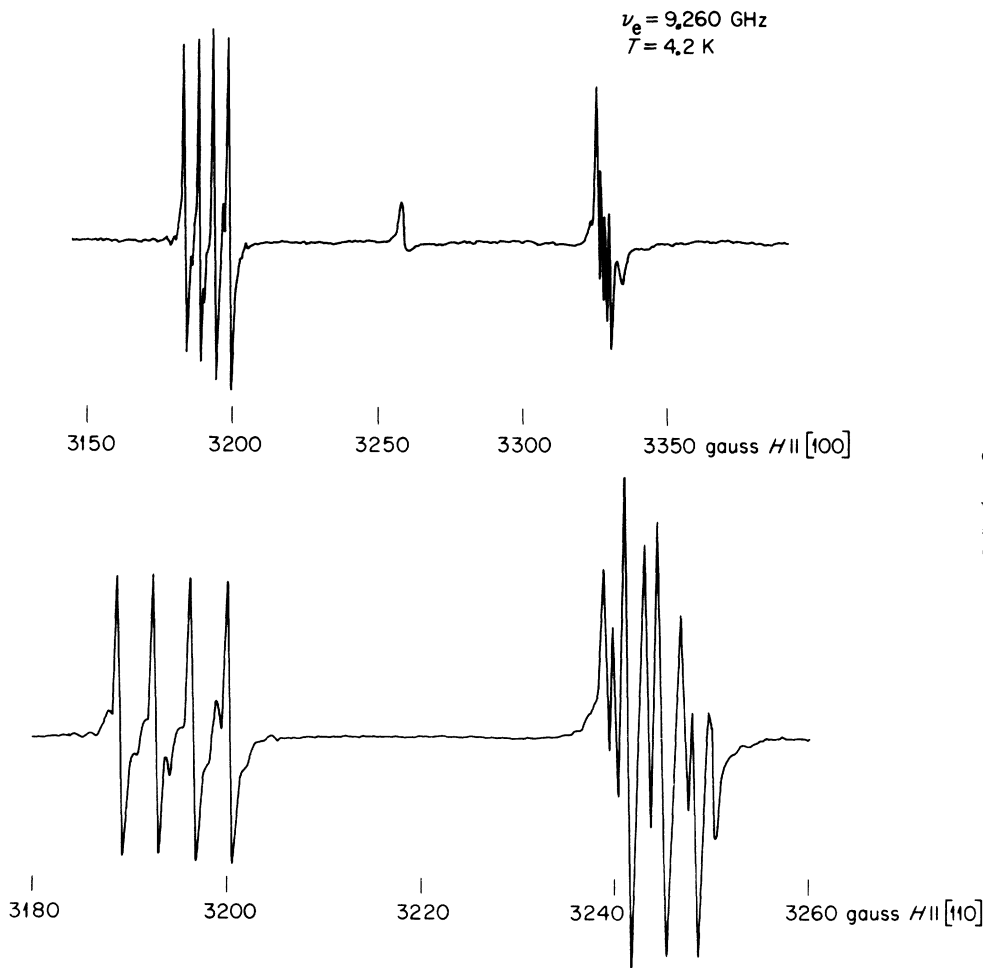


FIG. 1. EPR spectra of the $[\text{Na}]^0$ center in MgO . The upper trace with $\vec{H} \parallel [100]$ shows $\theta = 0^\circ$ and $\theta = 90^\circ$ groups. The lower trace with $\vec{H} \parallel [110]$ shows $\theta = 45^\circ$ and $\theta = 90^\circ$ groups.

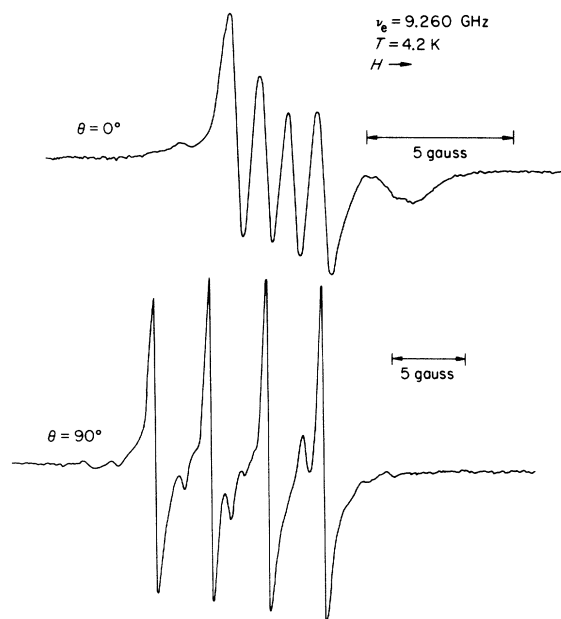


FIG. 2. EPR spectra of the $[\text{Na}]^0$ center in MgO with \vec{H} parallel and perpendicular to the defect axis.

measurement at a reference temperature, 4.2 K for the EPR and 77 K for the optical. The sample temperature was then rapidly raised to a given value for 7 min. Upon cooling to the reference temperature the spectrum was remeasured.

EXPERIMENTAL RESULTS

EPR

Figures 1-4 show the observed EPR spectra of

$\text{MgO}:\text{Na}$ and $\text{SrO}:\text{Na}$. From the angular variations it was concluded that in both lattices, the defect has $\langle 100 \rangle$ tetragonal symmetry. With the magnetic field parallel or perpendicular to the defect axis, there are clearly four major lines ($\Delta m_I = 0$) due to the hyperfine structure from the 100% naturally abundant ^{23}Na nucleus ($I = \frac{3}{2}$). When the field is not aligned along the defect axis, other lines of appreciable intensity appear which arise from the combined effects of the hyperfine, quadrupole, and nuclear Zeeman interactions. These additional lines may be seen in Figs. 1-3, where the spectra of the $[\text{Na}]^0$ center in MgO are displayed at various magnetic field orientations.

The appropriate spin Hamiltonian is

$$\mathcal{H} = \mu_B \vec{H} \cdot \vec{g} \cdot \vec{S} + \vec{I} \cdot \vec{A} \cdot \vec{S} + \vec{I} \cdot \vec{P} \cdot \vec{I} - g_N \mu_N \vec{H} \cdot \vec{I} ,$$

where all symbols have their usual significance.

The angular variation of the spectra shows that the tensors are all axial about the $\langle 100 \rangle$. A least-squares computer program was employed to evaluate the spin-Hamiltonian parameters using only the data obtained with the magnetic field parallel and perpendicular to the defect axis. Only the "allowed" $\Delta m_I = 0$ transitions were utilized, which eliminates the nuclear Zeeman term, and the results are tabulated in Table I. A more precise determination could be made by utilizing all the data from all the angles, but in view of the smallness of these parameters, this would be achieved with a greater economy of effort using electron-nuclear-double-resonance techniques. Also tabulated in Table I is the decomposition of the hyperfine tensor into its isotropic and anisotropic components, namely,

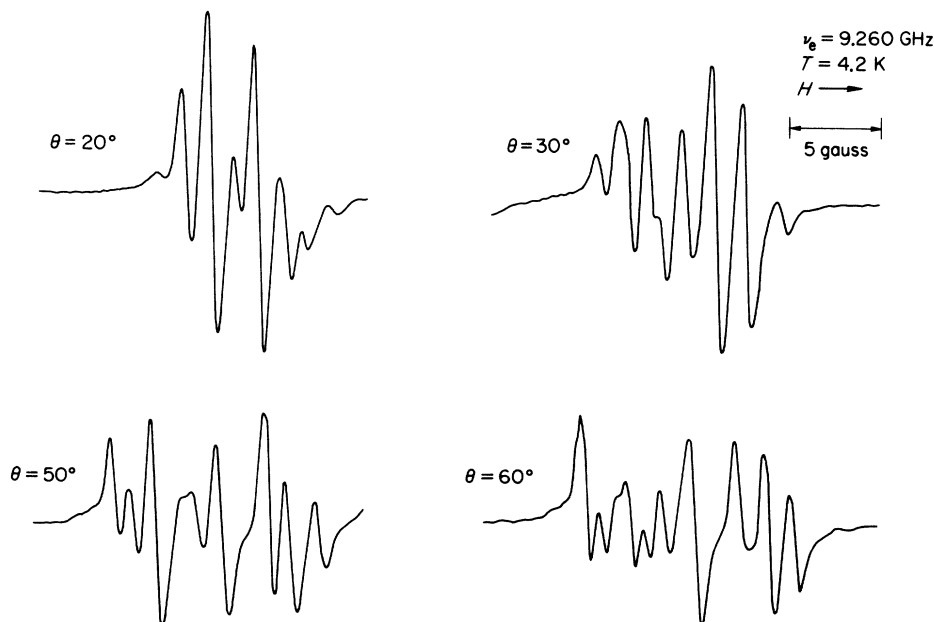


FIG. 3. EPR spectra of the $[\text{Na}]^0$ center in MgO with \vec{H} at various angles to the defect axis. The spectrum is complicated by additional lines due to the apparent breakdown of selection rules arising from the combined effects of hyperfine, quadrupole, and nuclear Zeeman interactions.

$A_{||} = a + 2b$ and $A_{\perp} = a - b$. It is interesting to note that the isotropic portion a for $[\text{Na}]^0$ is larger than that observed for $[\text{Li}]^0$,^{6,7} and that the anisotropic portion b is of different sign than a for $[\text{Li}]^0$ and $[\text{Na}]^0$ in all three alkaline earth oxides, MgO, CaO, and SrO. Finally, V^- -center lines were present in MgO:Na but not in SrO:Na. The latter, however, contained Na-aggregate centers, which have not been studied in detail.

Optical Absorption Bands

The spectra of sodium-doped MgO and SrO crystals consisted of broad overlapping bands originating from various radiation-induced defects. Fortunately, these defects display decay temperatures sufficiently distinct to permit separation of the $[\text{Na}]^0$ -center spectra by comparison of ESR and optical data at various stages of isochronal annealing.

MgO:Na

The EPR spectrum showed that there are two defects present, the $[\text{Na}]^0$ and V^- centers. Isochronal annealing indicates that at 232 K the former are annealed out, while the V^- centers remained essentially unchanged. The optical absorption spectrum of the same crystals consists mainly of two broad overlapping bands, as shown in Fig. 5. Indeed, after annealing at 240 K, a band peaking at 2.3 eV, that of the V^- centers, remained. Subtraction of this band from the initial composite spectrum yields a band peaking at 1.58 eV. This resultant band, representing the defects annealed out, is attributed to $[\text{Na}]^0$ centers in MgO. The half-width of this $[\text{Na}]^0$ band, 0.7–0.8 eV, is smaller than the ~1.0-eV half-width for the V^- band. An annealing study showed that the $[\text{Na}]^0$ band decays at 190 K.

SrO:Na

The EPR spectrum showed that $[\text{Na}]^0$ centers and aggregates of sodium ions were present. The $[\text{Na}]^0$ centers begin to decay at 132 K. At 186 K they are no longer stable, while substantial concentrations of the aggregate centers still remain. The optical spectrum of the same crystals also exhibited composite bands, shown in Fig. 6. The lower curve, obtained by subtracting the curve after annealing at 186 K from the composite band, represents contributions from defects annealed out. Peaks at 3.05 and 1.34 eV resulted. Of these, the 1.34-eV band is attributed to the $[\text{Na}]^0$ centers. The converse association is ruled out because the 186-K anneal decreased the 3.05-eV band only by a factor of 3, whereas the EPR spectrum indicated that the $[\text{Na}]^0$ centers were completely destroyed. The 1.34-eV band was found to decay at 160 K.

TABLE I. Spin-Hamiltonian parameters of hole centers in MgO, CaO, and SrO.

	$g_{ }$	g_{\perp}	$A_{ }$ (MHz)	B_{\perp} (MHz)	a (MHz)	b (MHz)	P (MHz)	Ref.
V^-	2.0032	2.0385	a
MgO $[\text{Li}]^0$	2.0043 ± 0.0003	2.0542 ± 0.0003	$\pm 0.56 \pm 0.14$	$\pm 6.97 \pm 0.06$	$\pm 4.80 \pm 0.10$	$\pm 2.12 \pm 0.10$...	b
MgO $[\text{Na}]^0$	2.0055 ± 0.0005	2.0721 ± 0.0005	$\pm 3.02 \pm 0.1$	$\pm 11.4 \pm 0.2$	± 8.61	± 2.79	$\approx \pm 0.8$	c
V^-	2.0011 ± 0.0004	2.0710 ± 0.0004	d
CaO $[\text{Li}]^0$	2.0019 ± 0.0005	2.0885 ± 0.0005	$\pm 0.006 \pm 0.05$	$\pm 3.87 \pm 0.02$	± 2.52	± 1.26	$\pm 0.0027 \pm 0.05$	b, e
CaO $[\text{Na}]^0$	2.0002 ± 0.0005	2.1234 ± 0.0005	$\pm 5.40 \pm 0.01$	$\pm 11.10 \pm 0.02$	± 9.14	± 1.84	$\pm 1.2 \pm 0.2$	e
V^-	2.0010 ± 0.0006	2.0703 ± 0.0006	f
SrO $[\text{Li}]^0$	1.9999 ± 0.0003	2.0931 ± 0.0003	0.0 ± 0.3	$\pm 2.8 \pm 0.3$	$\pm 1.8 \pm 0.3$	$\pm 0.9 \pm 0.3$...	b
SrO $[\text{Na}]^0$	1.9957 ± 0.0005	2.1454 ± 0.0005	$\pm 5.04 \pm 0.2$	$\pm 7.72 \pm 0.2$	± 6.83	± 0.89	$\pm 1.3 \pm 0.2$	c

^aReference 7.

^bJ. W. Culvahouse, L. V. Holroyd, and J. L. Kolopus, Phys. Rev. 140, A1181 (1965). These authors stated that the observed defect was probably the V^- center.

^cReference 1.

^dReference 6.

^eThis work.

^fReference 2.

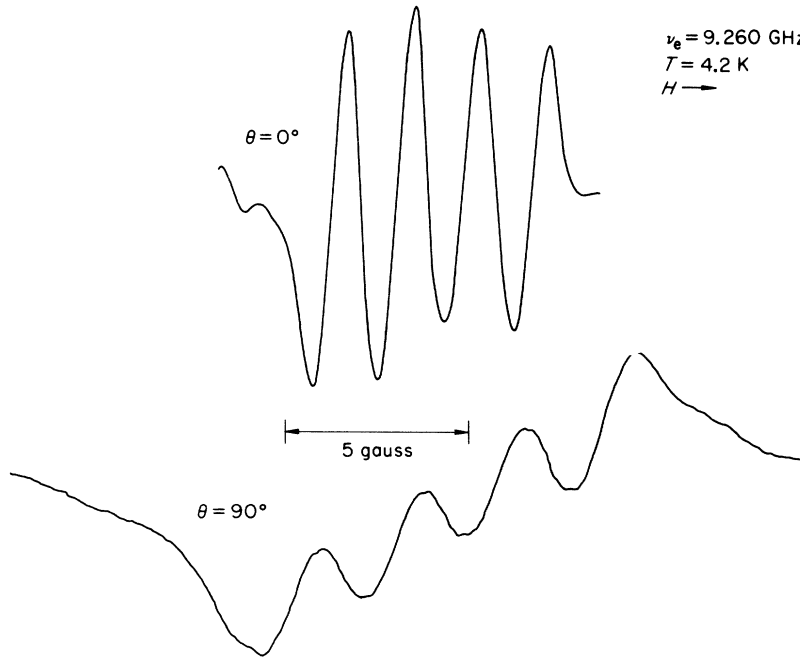


FIG. 4. EPR spectra of the $[\text{Na}]^0$ center in SrO with \vec{H} parallel and perpendicular to the defect axis.

DISCUSSION

It is evident that the introduction of a Na ion in a V^- -center site in MgO does not alter the symmetry

at low temperatures. However, it does shift the optical absorption peak from 2.3 eV of the V^- to the 1.58 eV of the $[\text{Na}]^0$ band. This decrease in peak energy falls short of the factor of 2 expected

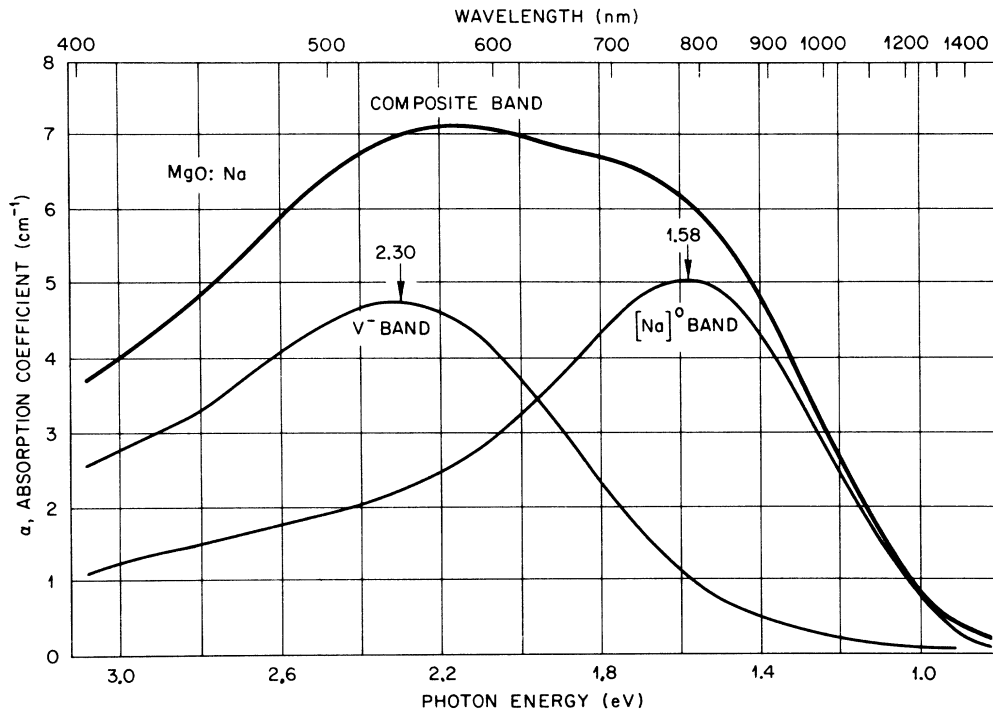


FIG. 5. Optical absorption spectrum of $\text{MgO}:\text{Na}$ after electron irradiation at 77 K. The band is shown decomposed experimentally (see text) into two separate bands with peaks at 2.30 and 1.58 eV.

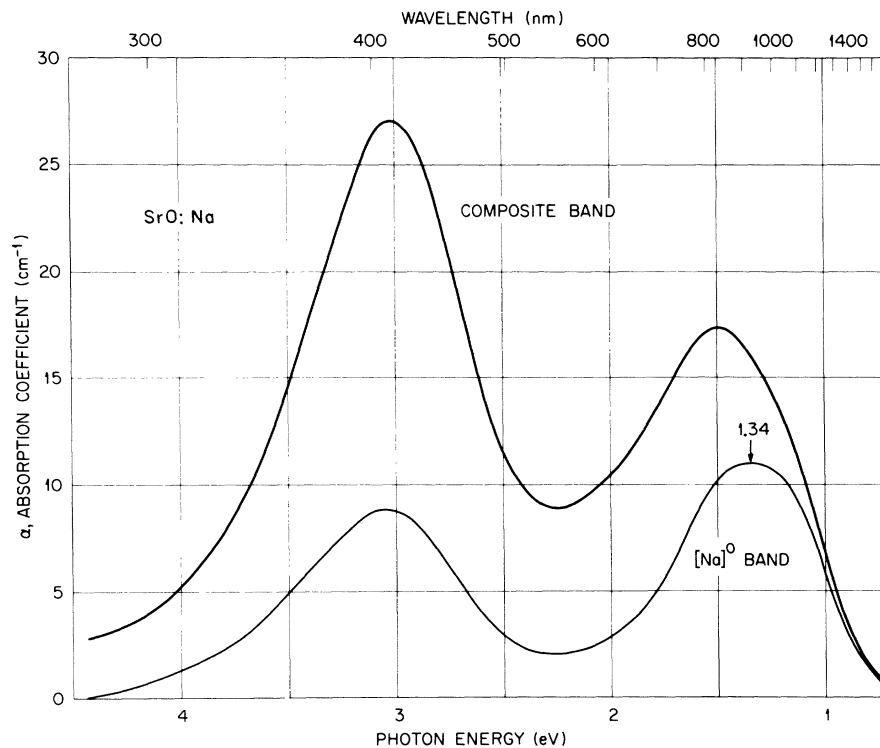


FIG. 6. Optical absorption spectrum of SrO:Na after electron irradiation at 77 K (upper curve). The lower curve corresponds to defects lost during isochronal annealing at 186 K (see text). The 1.34-eV peak is attributed to the $[\text{Na}]^0$ center.

from simple electrostatic potential considerations; that is, the effective charge as seen by the hole changes from -2 to -1 . A comparison of the optical bands in SrO is not possible, since the V^- band has yet to be observed. It should be mentioned that in this study no V^- center in SrO was detected, whereas 4×10^{17} - cm^{-3} V^- centers were observed in MgO. In addition, even though both MgO and SrO were exposed to the same amount of sodium dopants, they are less readily accepted in MgO than in SrO, owing to the large discrepancy in ionic size between the Na and Mg ions. This is shown by the large concentrations of both $[\text{Na}]^0$ and Na-aggregate centers observed in SrO, whereas relatively lower amounts of $[\text{Na}]^0$ centers and no aggregate centers were detected in MgO.

We shall apply our results to the model described previously.^{6,10,11} Its salient features are as follows: The hole is trapped at an oxygen nearest neighbor of the alkali ion forming an O^- . The threefold-degenerate $2p$ state of the free O^- ion is split by the tetragonal crystalline electric field into a doublet excited (p_x, p_y) state and a ground singlet (p_z) state with an energy separation Δ . The observed optical absorptions have been assumed to arise from transitions between the ground singlet and the excited doublet states, and therefore are a direct measurement of Δ . Even though this transition between the pure p states is forbidden, it has been expected that suitable admixtures of other states

can be invoked to give a nonzero transition probability.

The g values of the ground state are given by perturbation theory¹¹ as

$$g_{\perp} = 2.00232(1 - x - \frac{1}{2}x^2),$$

$$g_{\parallel} = 2.00232(1 - x^2),$$

where $x = \lambda / (\Delta - \frac{1}{2}\lambda)$ and λ is the spin-orbit coupling constant. Obviously, this states that g_{\parallel} will always be ≤ 2.00232 , which is not the case for the $[\text{Na}]^0$ center in MgO. Furthermore, using the experimental values of g_{\perp} and Δ , we find

$$\lambda = -834 \text{ cm}^{-1} \text{ for SrO}$$

$$= -461 \text{ cm}^{-1} \text{ for MgO.}$$

These are uncomfortably large compared to the expected free-ion value of $\lambda = -135 \text{ cm}^{-1}$. In addition, there is also the question of the relatively large oscillator strengths observed previously.⁷ However, it is possible that the observed optical absorption energy is not the Δ described in the model. The transition probability for the process involving a Δ may indeed be so small that it has escaped detection. If this is the case, then the origin of the observed optical bands need to be explained somehow. These problems constitute a serious challenge to the proposed model.

Perhaps other models should be given serious

considerations. In particular, the hole may be shared equally by the six nearest-neighbor oxygen ions which would, of course, exhibit cubic symmetry. To account for the observed axial symmetry, one may invoke a Jahn-Teller-type distortion. In

any event, it is apparent that the V^- , $[\text{Li}]^0$, and $[\text{Na}]^0$ defect centers are obviously similar in nature in MgO , CaO , and SrO , and presumably the correct model would have to account for the properties of this entire class of defect centers.

†Research sponsored by the U. S. Atomic Energy Commission under contract with Union Carbide Corp.

*Deceased.

‡Guest Scientist from University of Alabama, Birmingham, Ala.

¹J. E. Wertz, P. Auzins, J. H. E. Griffiths, and J. W. Orton, *Discussions Faraday Soc.* **28**, 136 (1959).

²A. J. Shuskus, *J. Chem. Phys.* **39**, 849 (1963).

³J. L. Kolopus, Ph.D. thesis (University of Missouri, Columbia, 1965) (unpublished); J. T. Suss, Ph.D. thesis (Hebrew University, Jerusalem, 1966) (unpublished).

⁴J. E. Wertz, G. S. Saville, P. Auzins, and J. W. Orton, *J. Phys. Soc. Japan Suppl.* **18**, 305 (1963).

⁵Y. Chen and W. A. Sibley, *Phys. Rev.* **154**, 842 (1967).

⁶O. F. Schirmer, *J. Phys. Chem. Solids* **32**, 499 (1971).

⁷H. T. Tohver, B. Henderson, Y. Chen, and M. M. Abraham, *Phys. Rev. B* (to be published).

⁸W. A. Sibley, J. L. Kolopus, and W. C. Mallard, *Phys. Status Solidi* **31**, 223 (1969).

⁹M. M. Abraham, C. T. Butler, and Y. Chen, *J. Chem. Phys.* **55**, 3752 (1971).

¹⁰W. E. Hagston, *J. Phys. C* **3**, 1233 (1970).

¹¹A. E. Hughes and B. Henderson, in *Defects in Crystalline Solids*, edited by J. H. Crawford, Jr., and L. M. Slifkin (Plenum, New York, 1971), and references therein.

Lattice Dynamics of Pyrolytic Graphite*

R. Nicklow, N. Wakabayashi, and H. G. Smith

Solid State Division, Oak Ridge National Laboratory, Oak Ridge, Tennessee 37830

(Received 3 December 1971)

The frequencies of certain normal modes of vibration of the graphite lattice have been studied on samples of high-quality pyrolytic graphite by coherent, inelastic-neutron-scattering techniques. Some of the data are not compatible with certain restrictions imposed by the valence-bond model as presented by Young and Koppel. Therefore, the data have been analyzed in terms of a simple axially symmetric, Born-von Kármán force-constant model. The results show that appreciable interactions exist between third nearest neighbors in the basal plane. The force model has been used to calculate a frequency distribution function and the lattice specific heat of graphite. These calculations are in excellent agreement with the specific heat measured for natural graphite in the temperature range 1.5–300°K.

I. INTRODUCTION

It is well known that the forces between the atoms in graphite are extremely anisotropic¹⁻⁴; those between adjacent basal planes are about two orders of magnitude smaller than the forces between neighboring atoms in the same plane, which are comparable to the exceptionally strong interatomic forces existing in diamond. In fact these interplanar forces are so weak that it is necessary to handle a crystalline graphite sample carefully in order to avoid cracking it or cleaving flakes from its (001) faces. Consequently, the vibrational modes, which correspond to the displacements of atoms relative to others on the same basal plane, have very high frequencies, whereas modes in which the basal planes move essentially as rigid units have quite low frequencies.

These lower-frequency modes were studied with neutron-coherent-inelastic-scattering techniques by Dolling and Brockhouse.⁵ The major difficulty of any such study on graphite is the lack of large single-crystal samples. At present only pyrolytic graphite samples consisting of very thin ($\sim 1 \mu$) graphite crystallites randomly oriented about a common c axis are available. Thus, as discussed by Dolling and Brockhouse,⁵ essentially the only portion of the phonon dispersion relation that can be studied unambiguously by coherent-neutron-scattering measurements is that corresponding to the longitudinal modes propagating along the [001] direction. However, they were able to obtain limited information about the lowest-frequency transverse modes propagating along the same direction.

Since the time of this earlier work the quality of pyrolytic graphite has improved considerably. It is